Acta Cryst E
CRYSTALLOGRAPHIC COMMUNICATIONS

ISSN 2056-9890

Received 3 March 2016
Accepted 18 April 2016

Edited by M. Zeller, Purdue University, USA

Keywords: crystal structure; manganese; oxalate bridge; coordination polymer.

CCDC reference: 1474882

Supporting information: this article has supporting information at journals.iucr.org/e

Crystal structure and spectroscopic analysis of a new oxalate-bridged Mn^{II} compound: *catena*-poly[guanidinium [[aquachloridomanganese(II)]-μ_2-oxalato-$\kappa^4O^1,O^2:O^{1'},O^{2'}$] monohydrate]

Hiba Sehimi,[a,b] Ichraf Chérif[a,b] and Mohamed Faouzi Zid[a]*

[a]Laboratoire de Matériaux et Cristallochimie, Faculté des Sciences de Tunis, Université de Tunis El Manar, 2092 Manar II Tunis, Tunisia, and [b]Université de Gabès, Faculté des Sciences de Gabès, Campus Universitaire, Cité Erriadh Zrig, Gabès, 6072, Tunisia. *Correspondence e-mail: faouzi.zid@fst.rnu.tn

As part of our studies on the synthesis and the characterization of oxalate-bridged compounds *M*–ox–*M* (ox = oxalate dianion and *M* = transition metal ion), we report the crystal structure of a new oxalate-bridged Mn^{II} phase, $\{(CH_6N_3)[Mn(C_2O_4)Cl(H_2O)]\cdot H_2O\}_n$. In the compound, a succession of Mn^{II} ions (situated on inversion centers) adopting a distorted octahedral coordination and bridged by oxalate ligands forms parallel zigzag chains running along the *c* axis. These chains are interconnected through O—H···O hydrogen-bonding interactions to form anionic layers parallel to (010). Individual layers are held together *via* strong hydrogen bonds involving the guanidinium cations (N—H···O and N—H···Cl) and the disordered non-coordinating water molecule (O—H···O and O—H···Cl), as well as by guanidinium π–π stacking. The structural data were confirmed by IR and UV–Visible spectroscopic analysis.

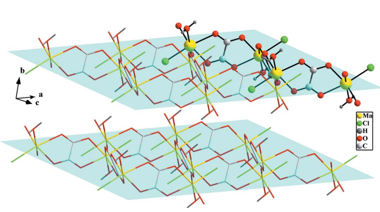

1. Chemical context

Much attention had been devoted to the coordination chemistry of oxalate (ox) anions due to the interesting structural features and physical properties they possess (Chérif *et al.*, 2011; Dridi *et al.*, 2013; Decurtins *et al.*, 1997). Oxalate anions have been demonstrated to be one of the most versatile bridging ligands for the construction of coordination polymers when combined with transition metal cations. Manganese(II) is a promising cation with possibilities of forming one-dimensional oxalato-based coordination polymers, as evidenced by reports describing the structures of several topologically similar Mn^{II}–ox–Mn^{II} chains [see, for example, García-Couceiro *et al.* (2005) or Beznischenko *et al.* (2009)]. In those compounds, the oxalate-bridged manganese framework may be considered as a single-chain magnet based on the oxalate linker (*e.g.* Clemente-León *et al.*, 2011). In this work, we report the synthesis and crystal structure determination of a new oxalate-bridged coordination compound, $\{(CH_6N_3)[Mn(C_2O_4)Cl(H_2O)]\cdot H_2O\}_n$ (I).

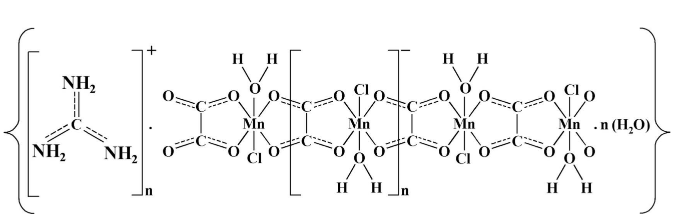

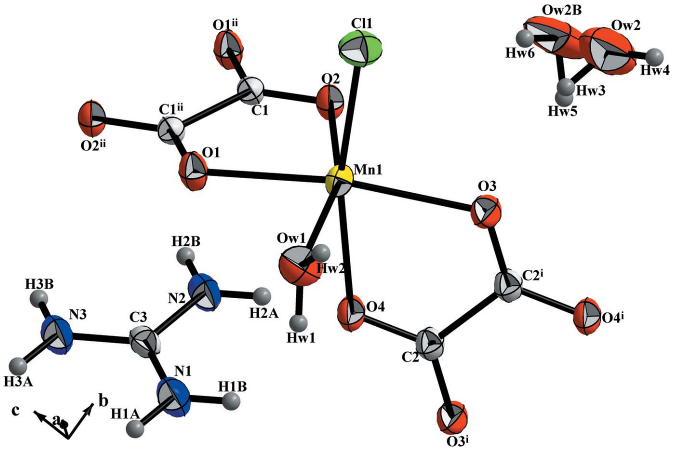

Figure 1
The structural unit of (I), showing the atom-numbering scheme. Displacement ellipsoids are drawn at the 50% probability level for non-H atoms. [Symmetry codes: (i) $-x + 1, -y + 1, -z + 1$; (ii) $-x + 1, -y + 1, -z$.]

2. Structural commentary

The principal structural motifs of the title compound are the complex anion $[MnCl(C_2O_4)(H_2O)]^-$, the organic cation $(CH_6N_3)^+$ and one disordered non-coordinating water molecule. A bond-valence-sum calculation, assuming Mn—O and Mn—Cl bonds, gives a BVS value (Brown & Altermatt, 1985) of 2.05 (7), confirming the +II oxidation state of Mn and ensuring electrical neutrality of the formed unit. The coordination environment of the Mn^{II} ion involves two oxalate ligands exhibiting bis-chelating coordination modes, one chloride atom and one oxygen atom of the aqua ligand (Fig. 1) in a slightly distorted octahedral geometry. The small bite angles of the bis-chelating oxalate groups [73.99 (6)° for O3—Mn1—O4 and 75.35 (7)° for O1—Mn1—O2] and the extended Mn1—Cl1 bond [2.458 (2) Å] account for this distortion. The polyhedral distance and angle distortions, calculated from the Mn—O and Mn—Cl distances and O—Mn—O and O—Mn—Cl angles in the MnO_5Cl unit, were found to be $ID_d = 0.03$ (2) and $ID_a = 0.22$ (4)%, respectively (Baur, 1974; Wildner, 1992).

The equatorial plane of the MnO_5Cl octahedron is formed by atoms Mn1, O*W*1, O1, O2 and O3, with a calculated root-mean-square deviation of the fitted atoms of 0.1038 Å. The axial positions are occupied by the chloride atom [Mn1—Cl1 = 2.458 (2) Å] and one oxygen atom from the bridging oxalato group [Mn1—O4 = 2.248 (2) Å]. The two oxalato groups are almost perpendicular with a dihedral angle of 89.09 (6)°. The oxalate ion is located on an inversion center that also relates the two Mn atoms bonded to the oxalate ion with each other. The bridged metal ions are nearly coplanar with the oxalate plane with a mean deviation of 0.0147 (8) Å.

The Mn^{II} ion, as a d^5 high-spin system with a spherical electron distribution, has a limited number of commonly observed coordination geometries that are based on minimization of ligand–ligand repulsion. Among the Mn—O distances, the shortest are those involving an oxygen atom from the oxalate ion *trans* to another oxygen atom from the second oxalate ion. The range of these distances is 2.180 (1) to 2.194 (1) Å, which is in accord with those observed in other oxalate-bridged compounds such as one of the polymorphs of *catena*-poly[[diaquamanganese(II)]-μ-oxalato-$\kappa^4O^1,O^2:O^{1'},O^{2'}$] (Soleimannejad *et al.*, 2007). The Mn—O distances involving the oxygen atoms of the oxalate ion *trans* to the coordinating water molecule and *trans* to the chloride atom are slightly longer at 2.202 (2) and 2.248 (2) Å.

The view of the structure packing (Fig. 2) shows the layered structure based on anionic zigzag oxalate-bridged Mn^{II} chains running along the *c* axis. The intra-chain Mn···Mn distances through bridging oxalate are 5.695 (2) and 5.778 (2) Å, somewhat longer than the value of 5.652 Å previously observed for $\{[Mn(C_2O_4)(C_8H_7N_3)]\cdot1.5H_2O\}_n$ (An & Zhu, 2009) involving a pyridyl-pyrazolide ligand instead of chloride

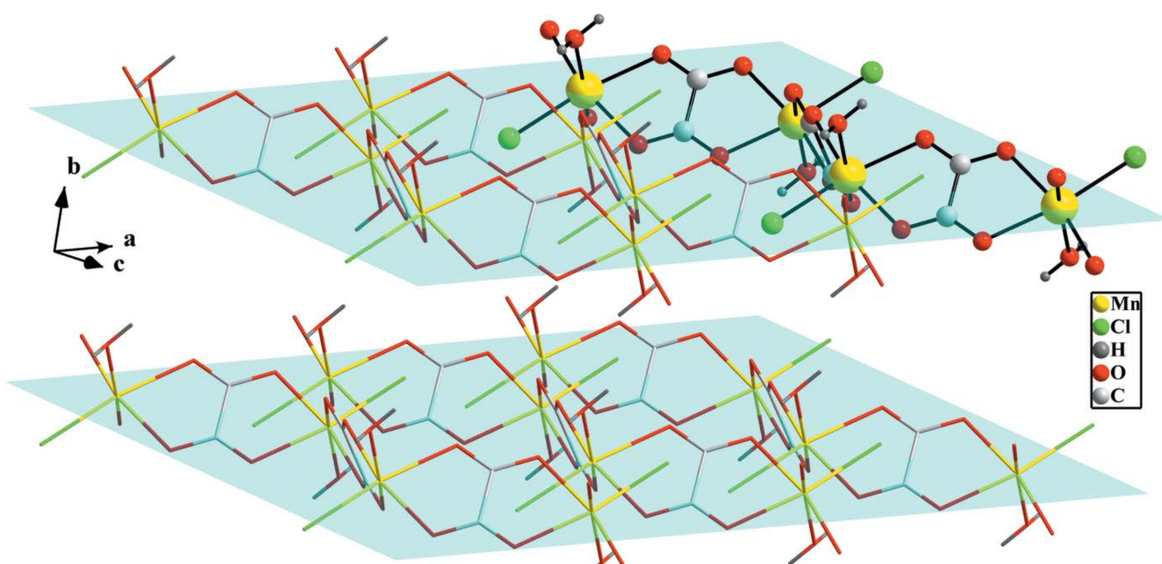

Figure 2
View of the structure packing showing Mn–Ox–Mn chains (highlighted by a ball-and-stick model) and layers parallel to (010) (blue planes).

and aqua ligands in the coordination environment of the Mn^{II} ion.

The geometric parameters for the guanidinium cations do not show any unusual features and are in agreement with those previously reported (Sakai *et al.* 2003; Vaidhyanathan *et al.*, 2001). The bond lengths [1.318 (2)–1.329 (2) Å] and angles [119.27 (16)–120.57 (16)°] are in the typical ranges, confirming a highly resonance-stabilized electronic structure and a completely delocalized charge between the three sp^2 nitrogen atoms. Conjugation of the nitrogen lone pairs with the empty *p*-orbital of the sp^2 carbon atom creates a planar cation.

3. Supramolecular features

Neighbouring oxalate-bridged zigzag chains are connected with each other *via* O—H···O hydrogen bonds involving the coordinating water molecule. Its oxygen atom acts as a hydrogen-bond donor and establishes strong hydrogen bonds (Table 1) towards one of the oxalate oxygen atoms of a neighbouring chain (Fig. 3), *O*W1—*H*W2···O3^{v} [symmetry code: (v) $-x+2, -y+1, -z$], leading to the formation of anionic layers parallel to (010). A disordered non-coordinating water molecule acts as acceptor (Fig. 3) for the other hydrogen atom involving the coordinating water molecule *via* the hydrogen bonds *O*W1—*H*W1···*O*W2^{i} and *O*W1—H*W*1···*O*W2*B*^{i} [symmetry code: (i) $x, y-1, z$]. Both disorder components of the non-coordinating water molecules act as hydrogen-bond donors towards oxygen atom O3 (Fig. 3) *via* the hydrogen bonds *O*W2—*H*W3···O3 and *O*W2*B*—*H*W5···O3, but they form different hydrogen bonds *via* their second H atom, to chlorine atoms in different lattice positions *via* hydrogen bonds *O*W2—*H*W4···Cl1^{vi} and *O*W2*B*-–*H*W6···Cl1 [symmetry code: (vi) $-x+2, -y+2, -z$]. The combined water hydrogen bonds link the anionic layers into a 3D framework.

Table 1
Hydrogen-bond geometry (Å, °).

D—H···*A*	*D*—H	H···*A*	*D*···*A*	*D*—H···*A*
N1—H1*A*···O2^{i}	0.86	2.19	3.047 (3)	175
N1—H1*B*···O4	0.86	2.20	2.917 (3)	140
N2—H2*A*···Cl1^{ii}	0.86	2.85	3.509 (3)	135
N2—H2*B*···Cl1^{iii}	0.86	2.56	3.357 (2)	154
N2—H2*A*···O4	0.86	2.38	3.054 (3)	135
N3—H3*A*···O1^{iv}	0.86	2.00	2.854 (3)	172
N3—H3*B*···Cl1^{iii}	0.86	2.57	3.363 (3)	154
*O*W1—HW1···*O*W2^{i}	0.85 (1)	1.96 (1)	2.793 (4)	170 (3)
*O*W1—HW1···*O*W2*B*^{i}	0.85 (1)	1.82 (2)	2.643 (11)	165 (3)
*O*W1—HW2···*O*3^{v}	0.84 (1)	2.06 (1)	2.890 (3)	176 (3)
*O*W2—HW3···O3	0.85 (1)	2.18 (2)	3.005 (5)	165 (5)
*O*W2—HW4···Cl1^{vi}	0.85 (1)	2.61 (3)	3.319 (6)	142 (4)
*O*W2*B*—HW5···O3	0.85 (1)	2.42 (11)	2.840 (10)	112 (9)
*O*W2*B*—HW6···Cl1	0.86 (1)	2.81 (1)	3.656 (18)	172 (11)

Symmetry codes: (i) $x, y-1, z$; (ii) $x-1, y, z$; (iii) $-x+1, -y+1, -z+1$; (iv) $-x+1, -y, -z+1$; (v) $-x+2, -y+1, -z$; (vi) $-x+2, -y+2, -z$.

The three N atoms of the guanidinium cation act as donors of hydrogen bonds N1—H1*A*···O2^{i}, N1—H1*B*···O4, N2—H2*A*···Cl1^{ii}, N2—H2*B*···Cl1^{iii}, N2—H2*A*···O4, N3—H3*A*···O1^{iv} and N3—H3*B*···Cl1^{iii} [Table 1; symmetry codes: (i) $x, y-1, z$; (ii) $x-1, y, z$; (iii) $-x+1, -y+1, -z+1$; (iv) $-x+1, -y, -z+1$], consolidating the anionic layers and giving additional stability to the three-dimensional structure as illustrated in Fig. 4. The guanidinium cations are also paired

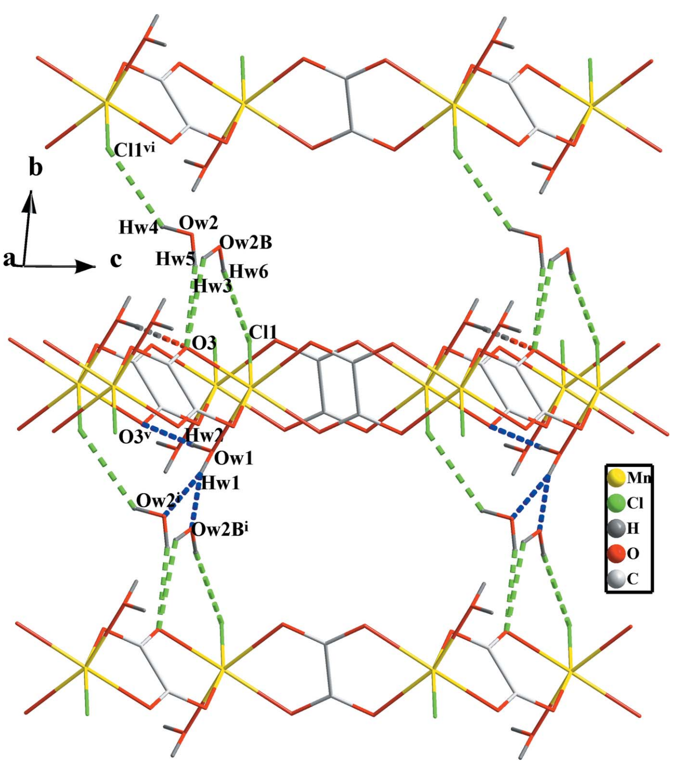

Figure 3
View of the hydrogen bonds developed by both coordinating (blue dashed lines) and non-coordinating (green dashed lines) water molecules. [Symmetry codes: (i) $x, y-1, z$; (v) $-x+2, -y+1, -z$; (vi) $-x+2, -y+2, -z$.]

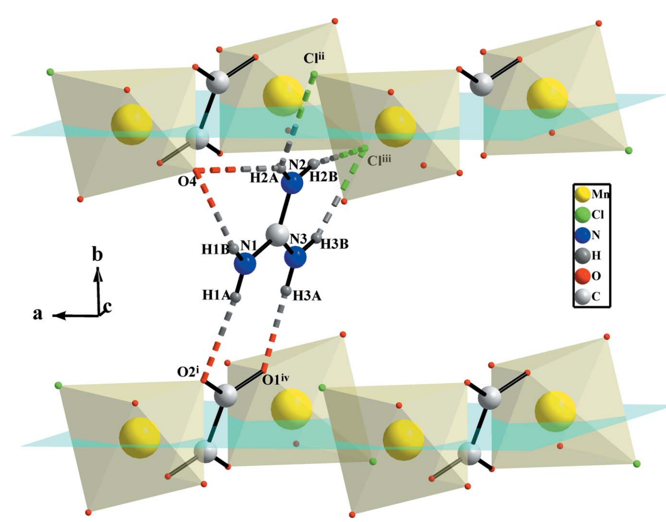

Figure 4
N—H···O and N—H···Cl hydrogen-bonding interactions developed by the guanidinium cations (dashed lines) in (I). Non-coordinating water molecules and hydrogen atoms of coordinating water molecules are omitted for clarity. [Symmetry codes: (i) $x, y-1, z$; (ii) $x-1, y, z$; (iii) $-x+1, -y+1, -z+1$; (iv) $-x+1, -y, -z+1$.]

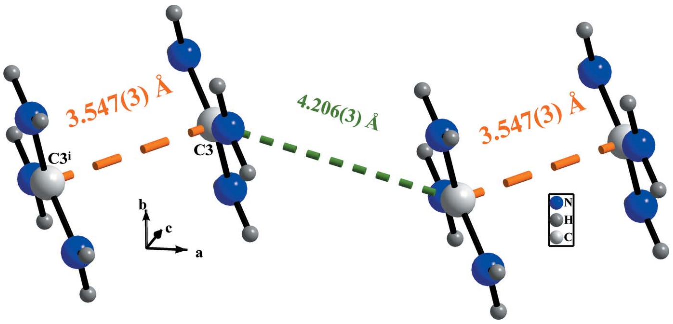

Figure 5
π–π stacking interactions (orange dashed lines) between adjacent organic cations. [Symmetry code: (i) $-x$, $-y$, $-z$ + 1.]

via π–π stacking with an interplanar distance of 3.547 (3) Å between C3 and C3($-x$, $-y$, $-z$ + 1) (Di Tondo & Pritchard, 2012), as shown in Fig. 5.

Table 2
IR data (cm^{-1}) for (I).

Wavenumber	Assignment
521	ν(Mn—Cl)
605	ν(Mn—O)
793	δ(COO)
1312, 1409	ν_s(COO)
1657	ν_{as}(COO)
2352	ν(N—H···O)
3182	$\nu_s(NH_2)$
3390	$\nu(OH)(H_2O)$ / $\nu_{as}(NH_2)$

Table 3
UV–Vis data (nm) for (I).

Wavelength	Assignment
206	$\pi \rightarrow \pi^*$
240	MLCT
329	$n \rightarrow \pi^*$

4. IR and UV–Vis characterizations

The IR spectrum was recorded in the 4000–400 cm^{-1} region using a Perkin–Elmer spectrometer with the sample diluted in a pressed KBr pellet. The most intense IR absorption bands of (I) are given in Table 2. The spectrum (Fig. 6) displays broad and strong bands centered at 3390 and 3182 cm^{-1} assigned to [ν(O—H) + $\nu_{as}(NH_2)$] and $\nu_s(NH_2)$, respectively (Sasikala *et al.*, 2015). The broadness of these bands is indicative of the presence of both coordinating and non-coordinating water molecules, as well as –NH_2 groups involved in an extensive hydrogen-bond framework, in agreement with the crystal structure. A weak band observed at 2352 cm^{-1} is attributed to an N—H···O stretching mode. The characteristic vibrations of the bridging oxalato ligand are observed at 1657 cm^{-1} [ν_{as}(COO)], 1312 and 1409 cm^{-1} [ν_s(COO)] and 793 cm^{-1} [δ(COO)] (Ma *et al.*, 2007). All these bands are consistent with the literature for a bis-chelating coordination of the oxalato ligand. Additional bands observed at around 605 and 521 cm^{-1} can be attributed to ν(Mn—Cl) (Zgolli *et al.*, 2011) and ν(Mn—O) (Biradar & Mruthyunjayaswamy, 2013), respectively.

Some crystals, selected under the microscope, were dissolved in 10 cm^3 of distilled water. The solution obtained was analyzed using a UV–Visible spectrometer. The spectrum of (I) (Table 3 and Fig. 7) shows significant transitions at 206 nm (with a shoulder at 240 nm) and 329 nm. The first band is due to the $\pi \rightarrow \pi^*$ transition of the guanidinium π system (Hoffmann *et al.*, 2009), the second witnesses the metal-to-ligand charge-transfer (Sun *et al.*, 1996) and the last corresponds to the $n \rightarrow \pi^*$ transition (Sasikala *et al.*, 2015). An examination of the visible region of the spectrum does not reveal obvious *d*–*d* transitions (insert of Fig. 7) which may be

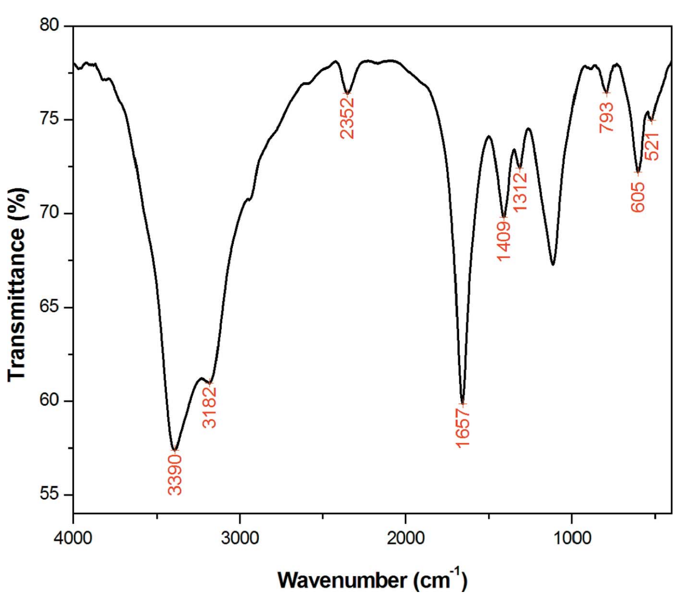

Figure 6
The IR spectrum of (I) in KBr.

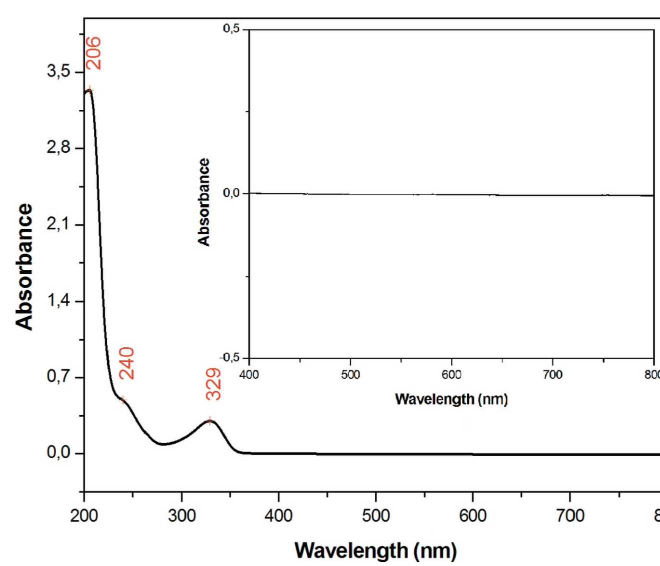

Figure 7
The UV–Vis spectrum of (I) in water. The insert is an expansion of the visible region.

Table 4
Experimental details.

Crystal data	
Chemical formula	$(CH_6N_3)[Mn(C_2O_4)Cl(H_2O)]\cdot H_2O$
M_r	274.53
Crystal system, space group	Triclinic, $P\bar{1}$
Temperature (K)	298
a, b, c (Å)	6.740 (5), 7.514 (7), 9.810 (2)
α, β, γ (°)	84.46 (3), 78.15 (4), 88.57 (6)
V (Å^3)	484.0 (6)
Z	2
Radiation type	Mo $K\alpha$
μ (mm^{-1})	1.65
Crystal size (mm)	0.50 × 0.43 × 0.34
Data collection	
Diffractometer	Enraf–Nonius CAD-4
Absorption correction	ψ scan (North *et al.*, 1968)
T_{min}, T_{max}	0.551, 0.718
No. of measured, independent and observed [$I > 2\sigma(I)$] reflections	4226, 2114, 2018
R_{int}	0.016
$(\sin \theta/\lambda)_{max}$ (Å^{-1})	0.638
Refinement	
$R[F^2 > 2\sigma(F^2)]$, $wR(F^2)$, S	0.024, 0.065, 1.10
No. of reflections	2114
No. of parameters	155
No. of restraints	11
H-atom treatment	H-atom parameters not refined
$\Delta\rho_{max}$, $\Delta\rho_{min}$ (e Å^{-3})	0.39, −0.30

Computer programs: *CAD-4 EXPRESS* (Duisenberg, 1992), *XCAD4* (Harms & Wocadlo, 1995), *SHELXS97* (Sheldrick, 2008), *SHELXL2014* (Sheldrick, 2015), *DIAMOND* (Brandenburg, 2006), *WinGX* (Farrugia, 2012) and *publCIF* (Westrip, 2010).

too weak to be seen, as they are spin and Laporte forbidden, in accordance with the compound being almost colourless.

5. Synthesis and crystallization

Aqueous solutions of ammonium oxalate and guanidine hydrochloride were added to $Mn(SO_4)\cdot H_2O$ dissolved in 10 cm^3 of water in a 1:2:1 molar ratio. The resulting solution was left at room temperature and colourless crystals suitable for X-ray diffraction were obtained after two weeks of slow evaporation.

6. Refinement

Crystal data, data collection and structure refinement details are summarized in Table 4.

Guanidinium hydrogen atoms were positioned geometrically as riding atoms (N—H = 0.86 Å) using adequate HFIX instructions and refined with AFIX instructions. Hydrogen atoms of the coordinating water molecule were found in Fourier difference maps. O—H distances were restrained to a value of 0.85 (1) Å and H···H distances were restrained to a value of 1.387 (1) Å.

The oxygen atom of the non-coordinating water molecule had unusually high displacement parameters, and was refined as disordered over two alternative mutually exclusive positions. The solvent molecule may be considered as being located vertically between negative-charged anionic layers formed by hydrogen-bonded polymeric chains and located horizontally between positive-charged pairs of guanidinium cations. This pseudo-channel affects its hydrogen-bonding interactions, see the discussion in the first paragraph of the *Supramolecular features* section and Fig. 3, which may explain the observed disorder.

The disordered oxygen atom was refined as disordered over two positions O*W*2 and O*W*2*B* which were restrained to have similar geometries. Their hydrogen atoms were located from the Fourier difference maps. The O—H bond lengths were restrained to a value of 0.85 (1) Å and the H···H distances were restrained to a value of 1.387 (1) Å. The interatomic distances between the two pairs O*W*2 and H*W*5 and O*W*2*B* and H*W*3 were restrained to be equal using a SADI instruction with an effective standard deviation of 0.02. The hydrogen-bonding distance of hydrogen atom H*W*6 to chlorine atom Cl1 was restrained to 2.80 (1) Å. Subject to these and the above conditions, the occupancy ratio of the disordered non-coordinating water molecule refined to 0.816 (13):0.184 (13).

Acknowledgements

Financial support from the Ministry of Higher Education and Scientific Research of Tunisia is gratefully acknowledged.

References

An, Z. & Zhu, L. (2009). *Acta Cryst.* E**65**, m1480.
Baur, W. H. (1974). *Acta Cryst.* B**30**, 1195–1215.
Beznischenko, A. O., Makhankova, V. G., Kokozay, V. N., Dyakonenko, V. V. & Shishkin, O. V. (2009). *Inorg. Chem. Commun.* **12**, 473–475.
Biradar, V. D. & Mruthyunjayaswamy, B. H. M. (2013). *The Scientific World Journal*, pp. 1–13.
Brandenburg, K. (2006). *DIAMOND*. Crystal Impact GbR, Bonn, Germany.
Brown, I. D. & Altermatt, D. (1985). *Acta Cryst.* B**41**, 244–247.
Chérif, I., Abdelhak, J., Zid, M. F. & Driss, A. (2011). *Acta Cryst.* E**67**, m1648–m1649.
Clemente-León, M., Coronado, E., Martí-Gastaldo, C. & Romero, F. M. (2011). *Chem. Soc. Rev.* **40**, 473–497.
Decurtins, S., Schmalle, H. W., Pellaux, R., Fischer, P. & Hauser, A. (1997). *Mol. Cryst. Liq. Cryst.* **305**, 227–237.
Di Tondo, P. & Pritchard, R. G. (2012). *Acta Cryst.* C**68**, i50–i52.
Dridi, R., Namouchi Cherni, S., Zid, M. F. & Driss, A. (2013). *Acta Cryst.* E**69**, m489–m490.
Duisenberg, A. J. M. (1992). *J. Appl. Cryst.* **25**, 92–96.
Farrugia, L. J. (2012). *J. Appl. Cryst.* **45**, 849–854.
García-Couceiro, U., Olea, D., Castillo, O., Luque, A., Román, P., de Pablo, P. J., Gómez-Herrero, J. & Zamora, F. (2005). *Inorg. Chem.* **44**, 8343–8348.
Harms, K. & Wocadlo, S. (1995). *XCAD4*. University of Marburg, Germany.
Hoffmann, A., Börner, J., Flörke, U. & Herres-Pawlis, S. (2009). *Inorg. Chim. Acta*, **362**, 1185–1193.
Ma, F.-X., Meng, F.-X., Liu, K., Pang, H.-J., Shi, D.-M. & Chen, Y.-G. (2007). *Transition Met. Chem.* **32**, 981–984.
North, A. C. T., Phillips, D. C. & Mathews, F. S. (1968). *Acta Cryst.* A**24**, 351–359.

Sakai, K., Akiyama, N., Mizota, M., Yokokawa, K. & Yokoyama, Y. (2003). *Acta Cryst.* E**59**, m408–m410.
Sasikala, V., Sajan, D., Sabu, K. J., Arumanayagam, T. & Murugakoothan, P. (2015). *Spectrochim. Acta A*, **139**, 555–572.
Sheldrick, G. M. (2008). *Acta Cryst.* A**64**, 112–122.
Sheldrick, G. M. (2015). *Acta Cryst.* C**71**, 3–8.
Soleimannejad, J., Aghabozorg, H., Hooshmand, S., Ghadermazi, M. & Attar Gharamaleki, J. (2007). *Acta Cryst.* E**63**, m2389–m2390.
Sun, X.-R., Miao, M.-M., Cheng, P., Liao, D. Z., Jiang, Z.-H. & Wang, G.-L. (1996). *Transition Met. Chem.* **21**, 270–272.
Vaidhyanathan, R., Natarajan, S. & Rao, C. N. R. (2001). *J. Chem. Soc. Dalton Trans.* pp. 699–706.
Westrip, S. P. (2010). *J. Appl. Cryst.* **43**, 920–925.
Wildner, M. (1992). *Z. Kristallogr.* **202**, 51–70.
Zgolli, D. Z., Boughzala, H. & Driss, A. (2011). *J. Soc. Chim. Tunis.* **13**, 173–178.

supporting information

Acta Cryst. (2016). E**72**, 724-729 [doi:10.1107/S2056989016006605]

Crystal structure and spectroscopic analysis of a new oxalate-bridged Mn^{II} compound: *catena*-poly[guanidinium [[aquachloridomanganese(II)]-μ_2-oxalato-$\kappa^4O^1,O^2:O^{1\prime},O^{2\prime}$] monohydrate]

Hiba Sehimi, Ichraf Chérif and Mohamed Faouzi Zid

Computing details

Data collection: *CAD-4 EXPRESS* (Duisenberg, 1992); cell refinement: *CAD-4 EXPRESS* (Duisenberg, 1992); data reduction: *XCAD4* (Harms & Wocadlo, 1995); program(s) used to solve structure: *SHELXS97* (Sheldrick, 2008); program(s) used to refine structure: *SHELXL2014* (Sheldrick, 2015); molecular graphics: *DIAMOND* (Brandenburg, 2006); software used to prepare material for publication: *WinGX* (Farrugia, 2012) and *publCIF* (Westrip, 2010).

catena-Poly[guanidinium [[aquachloridomanganese(II)]-μ_2-oxalato-$\kappa^4O^1,O^2:O^{1\prime},O^{2\prime}$] monohydrate]

Crystal data

$(CH_6N_3)[Mn(C_2O_4)Cl(H_2O)]\cdot H_2O$
M_r = 274.53
Triclinic, $P\bar{1}$
a = 6.740 (5) Å
b = 7.514 (7) Å
c = 9.810 (2) Å
α = 84.46 (3)°
β = 78.15 (4)°
γ = 88.57 (6)°
V = 484.0 (6) Å^3
Z = 2
$F(000)$ = 278
D_x = 1.884 Mg m^{-3}
Mo $K\alpha$ radiation, λ = 0.71073 Å
Cell parameters from 25 reflections
θ = 10–15°
μ = 1.65 mm^{-1}
T = 298 K
Prism, colourless
0.50 × 0.43 × 0.34 mm

Data collection

Enraf–Nonius CAD-4 diffractometer
Radiation source: fine-focus sealed tube
$\omega/2\theta$ scans
Absorption correction: ψ scan (North *et al.*, 1968)
T_{min} = 0.551, T_{max} = 0.718
4226 measured reflections
2114 independent reflections
2018 reflections with $I > 2\sigma(I)$
R_{int} = 0.016
θ_{max} = 27.0°, θ_{min} = 2.1°
h = −8→8
k = −9→9
l = −12→12
2 standard reflections every 120 reflections
intensity decay: 1.4%

Refinement

Refinement on F^2
Least-squares matrix: full
$R[F^2 > 2\sigma(F^2)]$ = 0.024
$wR(F^2)$ = 0.065
S = 1.10
2114 reflections
155 parameters
11 restraints
Primary atom site location: structure-invariant direct methods
Secondary atom site location: difference Fourier map

Hydrogen site location: inferred from neighbouring sites
H-atom parameters not refined

$w = 1/[\sigma^2(F_o^2) + (0.034P)^2 + 0.1929P]$
where $P = (F_o^2 + 2F_c^2)/3$
$(\Delta/\sigma)_{max} = 0.001$
$\Delta\rho_{max} = 0.39$ e Å^{-3}
$\Delta\rho_{min} = -0.30$ e Å^{-3}

Special details

Geometry. All esds (except the esd in the dihedral angle between two l.s. planes) are estimated using the full covariance matrix. The cell esds are taken into account individually in the estimation of esds in distances, angles and torsion angles; correlations between esds in cell parameters are only used when they are defined by crystal symmetry. An approximate (isotropic) treatment of cell esds is used for estimating esds involving l.s. planes.

Refinement. Refinement of F^2 against ALL reflections. The weighted R-factor wR and goodness of fit S are based on F^2, conventional R-factors R are based on F, with F set to zero for negative F^2. The threshold expression of $F^2 > 2\text{sigma}(F^2)$ is used only for calculating R-factors(gt) etc. and is not relevant to the choice of reflections for refinement. R-factors based on F^2 are statistically about twice as large as those based on F, and R- factors based on ALL data will be even larger.

Fractional atomic coordinates and isotropic or equivalent isotropic displacement parameters (Å^2)

	x	*y*	*z*	U_{iso}*/U_{eq}	Occ. (<1)
Mn1	0.72543 (3)	0.49656 (3)	0.22092 (2)	0.02231 (9)	
Cl1	1.03175 (7)	0.65970 (6)	0.23354 (5)	0.03534 (12)	
N2	0.1713 (2)	0.28093 (18)	0.43164 (16)	0.0312 (3)	
H2B	0.1064	0.3297	0.5036	0.037*	
H2A	0.1950	0.3411	0.3509	0.037*	
O4	0.47159 (18)	0.36133 (16)	0.15474 (12)	0.0285 (2)	
O2	0.50953 (17)	0.66001 (14)	0.35754 (11)	0.0247 (2)	
N1	0.3354 (3)	0.03734 (19)	0.33501 (16)	0.0351 (3)	
H1A	0.3768	−0.0715	0.3441	0.042*	
H1B	0.3592	0.0972	0.2542	0.042*	
O3	0.69372 (19)	0.63896 (16)	0.02047 (12)	0.0286 (2)	
O1	0.66931 (18)	0.34160 (15)	0.42455 (11)	0.0268 (2)	
OW1	0.9107 (2)	0.26878 (18)	0.14629 (14)	0.0367 (3)	
HW1	0.854 (3)	0.189 (3)	0.112 (2)	0.055*	
HW2	1.027 (2)	0.290 (3)	0.100 (2)	0.055*	
C1	0.4541 (2)	0.59228 (18)	0.48007 (15)	0.0198 (3)	
N3	0.1977 (2)	0.02218 (19)	0.56968 (16)	0.0326 (3)	
H3A	0.2386	−0.0867	0.5796	0.039*	
H3B	0.1323	0.0721	0.6409	0.039*	
C2	0.4359 (2)	0.41972 (19)	0.03918 (15)	0.0221 (3)	
C3	0.2351 (2)	0.1125 (2)	0.44522 (17)	0.0253 (3)	
OW2	0.7198 (6)	1.0392 (5)	0.0066 (7)	0.0831 (13)	0.816 (13)
HW3	0.719 (8)	0.9263 (18)	0.025 (5)	0.125*	0.816 (13)
HW4	0.793 (7)	1.067 (6)	−0.074 (3)	0.125*	0.816 (13)
OW2B	0.712 (2)	0.9962 (16)	0.089 (2)	0.061 (5)	0.184 (13)
HW5	0.637 (17)	0.955 (12)	0.039 (9)	0.091*	0.184 (13)
HW6	0.79 (2)	0.912 (12)	0.115 (14)	0.091*	0.184 (13)

Atomic displacement parameters (Å²)

	U^{11}	U^{22}	U^{33}	U^{12}	U^{13}	U^{23}
Mn1	0.02388 (14)	0.02454 (14)	0.01771 (13)	−0.00049 (9)	−0.00325 (9)	0.00002 (9)
Cl1	0.0292 (2)	0.0383 (2)	0.0387 (2)	−0.00641 (17)	−0.00517 (17)	−0.00671 (17)
N2	0.0365 (8)	0.0223 (6)	0.0341 (7)	0.0016 (6)	−0.0084 (6)	0.0032 (5)
O4	0.0324 (6)	0.0304 (6)	0.0219 (5)	−0.0077 (5)	−0.0073 (5)	0.0071 (4)
O2	0.0291 (6)	0.0231 (5)	0.0197 (5)	0.0029 (4)	−0.0024 (4)	0.0026 (4)
N1	0.0438 (9)	0.0241 (7)	0.0340 (8)	0.0004 (6)	−0.0024 (7)	0.0019 (6)
O3	0.0299 (6)	0.0319 (6)	0.0242 (5)	−0.0109 (5)	−0.0080 (5)	0.0039 (4)
O1	0.0327 (6)	0.0224 (5)	0.0217 (5)	0.0075 (4)	0.0008 (4)	0.0007 (4)
OW1	0.0333 (7)	0.0356 (7)	0.0377 (7)	0.0004 (5)	0.0032 (6)	−0.0080 (5)
C1	0.0211 (7)	0.0174 (7)	0.0208 (7)	−0.0008 (5)	−0.0048 (5)	0.0000 (5)
N3	0.0401 (8)	0.0230 (7)	0.0332 (7)	0.0021 (6)	−0.0074 (6)	0.0036 (6)
C2	0.0231 (7)	0.0222 (7)	0.0194 (7)	−0.0006 (6)	−0.0015 (6)	0.0000 (5)
C3	0.0244 (7)	0.0202 (7)	0.0326 (8)	−0.0043 (6)	−0.0101 (6)	0.0019 (6)
OW2	0.123 (3)	0.0459 (16)	0.076 (3)	−0.0154 (15)	−0.002 (2)	−0.0180 (19)
OW2B	0.078 (8)	0.031 (5)	0.067 (11)	−0.012 (5)	0.009 (6)	−0.020 (6)

Geometric parameters (Å, º)

Mn1—O1	2.1798 (14)	O1—C1^{ii}	1.251 (2)
Mn1—OW1	2.187 (2)	OW1—HW1	0.846 (9)
Mn1—O3	2.1936 (13)	OW1—HW2	0.835 (9)
Mn1—O2	2.2024 (18)	C1—O1^{ii}	1.251 (2)
Mn1—O4	2.2476 (19)	C1—C1^{ii}	1.552 (3)
Mn1—Cl1	2.4581 (19)	N3—C3	1.318 (2)
N2—C3	1.329 (2)	N3—H3A	0.8600
N2—H2B	0.8600	N3—H3B	0.8600
N2—H2A	0.8600	C2—O3^{i}	1.257 (2)
O4—C2	1.2434 (19)	C2—C2^{i}	1.547 (3)
O2—C1	1.2451 (19)	OW2—HW3	0.850 (10)
N1—C3	1.321 (2)	OW2—HW4	0.849 (10)
N1—H1A	0.8600	OW2B—HW5	0.851 (10)
N1—H1B	0.8600	OW2B—HW6	0.856 (10)
O3—C2^{i}	1.257 (2)		
O1—Mn1—OW1	85.68 (7)	C3—N1—H1B	120.0
O1—Mn1—O3	164.34 (5)	H1A—N1—H1B	120.0
OW1—Mn1—O3	100.06 (7)	C2^{i}—O3—Mn1	116.88 (11)
O1—Mn1—O2	75.35 (7)	C1^{ii}—O1—Mn1	116.15 (10)
OW1—Mn1—O2	160.68 (5)	Mn1—OW1—HW1	117.6 (17)
O3—Mn1—O2	97.39 (6)	Mn1—OW1—HW2	117.3 (17)
O1—Mn1—O4	92.12 (7)	HW1—OW1—HW2	111.4 (15)
OW1—Mn1—O4	85.45 (8)	O2—C1—O1^{ii}	126.35 (14)
O3—Mn1—O4	73.99 (6)	O2—C1—C1^{ii}	117.50 (16)
O2—Mn1—O4	91.49 (7)	O1^{ii}—C1—C1^{ii}	116.15 (16)
O1—Mn1—Cl1	100.46 (6)	C3—N3—H3A	120.0

OW1—Mn1—Cl1	90.50 (7)	C3—N3—H3B	120.0
O3—Mn1—Cl1	94.08 (6)	H3A—N3—H3B	120.0
O2—Mn1—Cl1	96.47 (7)	O4—C2—O3^{i}	126.48 (15)
O4—Mn1—Cl1	166.46 (3)	O4—C2—C2^{i}	116.80 (17)
C3—N2—H2B	120.0	O3^{i}—C2—C2^{i}	116.73 (16)
C3—N2—H2A	120.0	N3—C3—N1	120.57 (16)
H2B—N2—H2A	120.0	N3—C3—N2	119.27 (16)
C2—O4—Mn1	115.50 (11)	N1—C3—N2	120.16 (16)
C1—O2—Mn1	114.82 (10)	HW3—OW2—HW4	109.7 (17)
C3—N1—H1A	120.0	HW5—OW2B—HW6	108.7 (18)

Symmetry codes: (i) −*x*+1, −*y*+1, −*z*; (ii) −*x*+1, −*y*+1, −*z*+1.

Hydrogen-bond geometry (Å, º)

D—H···*A*	*D*—H	H···*A*	*D*···*A*	*D*—H···*A*
N1—H1*A*···O2^{iii}	0.86	2.19	3.047 (3)	175
N1—H1*B*···O4	0.86	2.20	2.917 (3)	140
N2—H2*A*···Cl1^{iv}	0.86	2.85	3.509 (3)	135
N2—H2*B*···Cl1^{ii}	0.86	2.56	3.357 (2)	154
N2—H2*A*···O4	0.86	2.38	3.054 (3)	135
N3—H3*A*···O1^{v}	0.86	2.00	2.854 (3)	172
N3—H3*B*···Cl1^{ii}	0.86	2.57	3.363 (3)	154
O*W*1—H*W*1···O*W*2^{iii}	0.85 (1)	1.96 (1)	2.793 (4)	170 (3)
O*W*1—H*W*1···O*W*2*B*^{iii}	0.85 (1)	1.82 (2)	2.643 (11)	165 (3)
O*W*1—H*W*2···O3^{vi}	0.84 (1)	2.06 (1)	2.890 (3)	176 (3)
O*W*2—H*W*3···O3	0.85 (1)	2.17 (2)	3.005 (5)	165 (5)
O*W*2—H*W*4···Cl1^{vii}	0.85 (1)	2.61 (3)	3.319 (6)	142 (4)
O*W*2*B*—H*W*5···O3	0.85 (1)	2.42 (11)	2.840 (10)	112 (9)
O*W*2*B*—H*W*6···Cl1	0.86 (1)	2.81 (1)	3.656 (18)	172 (11)

Symmetry codes: (ii) −*x*+1, −*y*+1, −*z*+1; (iii) *x*, *y*−1, *z*; (iv) *x*−1, *y*, *z*; (v) −*x*+1, −*y*, −*z*+1; (vi) −*x*+2, −*y*+1, −*z*; (vii) −*x*+2, −*y*+2, −*z*.